Circular Dichroic Triplet−Singlet Difference Spectroscopy. 1. Analysis of Dichroic Components in Optically Detected Magnetic Resonance

Gabrielle M. Owen and Arnold J. Hoff*

Department of Biophysics, Huygens Laboratory, Leiden University, P.O. Box 9504, 2300 RA Leiden, The Netherlands

Received: May 11, 1999; In Final Form: September 22, 1999

Linear and circular dichroic triplet-minus-singlet spectroscopy (LD(T−S) and CD(T−S)) are highly sensitive methods for determining the angles between the optical and microwave transition moments, the strength of molecular interactions, and band assignments of a wide range of biological systems. Both LD(T−S) and CD(T−S) spectra can in principle be measured via dichroic optically detected magnetic resonance (ODMR), a complex measurement method involving a sample with both linear and circular anisotropies, imperfect light modulation, possibly misaligned components, optical elements at low temperatures, and a partially polarized light source. We report a theoretical analysis of the influence of these effects on the measured spectra, via a Stokes−Mueller analysis of the optical system used for recording dichroic-ODMR spectra. From the theoretical results we develop and test experimental strategies to ensure the reliability and measurability of LD(T−S) and CD(T−S) spectra.

1. Introduction

For approximately the past 20 years optically detected magnetic resonance spectroscopy (ODMR)[24] has been used to investigate biological molecules, including the aromatic amino acids, the purine and pyrimidine bases of DNA and RNA, the photosynthetic pigments, and other protein-associated pigments such as flavines. ODMR is used to measure the change in an optical property due to microwave-induced transitions between magnetic sublevels of the lowest triplet state.[1,2] The three branches of ODMR are named after the commonly monitored optical properties: absorbance (ADMR), fluorescence (FDMR), and phosphorescence (PDMR). The strengths of ODMR are the intrinsic nature of the excited triplet state as a spin probe, the high sensitivity when optically detecting the magnetic resonance transitions, and the ability to select via the frequency of the oscillating magnetic field among triplets on different types of molecules and even on the same type of molecule in different environments.

Various types of triplet-minus-singlet (T−S) spectra can be measured with ADMR. The different T−S spectra show the subtle differences of the optical properties of the system in the singlet and triplet states, from which intermolecular distances, relative orientations, and couplings can be determined. The selection via the frequency of the magnetic field with ADMR results in a higher resolution and recording speed for T−S spectra than via the laser-flash technique. The T−S spectrum is the difference of the absorbance with and without the presence of a triplet, and likewise, the double difference linear dichroic T−S (LD(T−S)) or circular dichroic T−S (CD(T−S)) spectra are the difference of the LD or CD with and without the presence of a triplet. Thus the singlet parts of the T−S and CD(T−S) spectra at a fixed microwave frequency are selected subsets of the singlet absorbance and circular dichroism (CD) measured with conventional absorption spectroscopy. Note that the angle between the optical and microwave transition moments is derived from the ratio of the LD(T−S) signal to the T−S signal at low microwave powers, whereas the angle between the optical transition moment and the membrane normal or symmetry axis of sample is derived from the ratio of the LD to the absorbance signal. Both of these angles can be used to help derive the structure of the examined molecule and to definitely assign bands in the T−S spectra. CD(T−S) spectroscopy can be used to detect changes in excitonic interactions with and without the presence of the triplet state, which reveals information about the couplings of the interacting molecules. The high sensitivity of CD and CD(T−S) helps to identify bands which remain unresolved in absorbance spectra or T−S absorbance spectra. Unlike experimental LD(T−S) spectroscopy,[3−6] CD(T−S) spectroscopy has not yet been reported.

In two papers we introduce a theoretical analysis and an experimental demonstration of CD(T−S) spectroscopy using optically detected magnetic resonance. Since dichroic-ADMR is a complex method, involving a sample with both linear and circular anisotropies, imperfect light modulation, possibly misaligned components, and optical elements at low temperatures, the measurement system needs to be analyzed carefully in order to avoid dichroic artifacts, such as have been noted in LD and CD measurements[7−9] and in time-resolved CD measurements.[10] In the present paper we analyze the optical system via the Stokes−Mueller formalism.[11,12] In our upcoming paper we apply the strategies for minimizing the mixing of optical anisotropies developed here, and report the first experimental CD(T−S) spectra.

2. Theory

In this section we present four Mueller matrix analyses of the optical system used to measure LD- and CD-ADMR spectra. No consideration is taken for reflection, scattering, or nonlinear optical effects. In the Stokes−Mueller formalism the incident light is described by a vector of light intensities $\bar{s}_{in}$ and the optical elements by 4×4 linear operators, **M**. The effect of the optical elements on the polarization of the incoming light

* Corresponding author. E-mail: hoff@biophys. LeidenUniv.nl.

10.1021/jp9915580 CCC: $18.00
Published on Web 11/18/1999

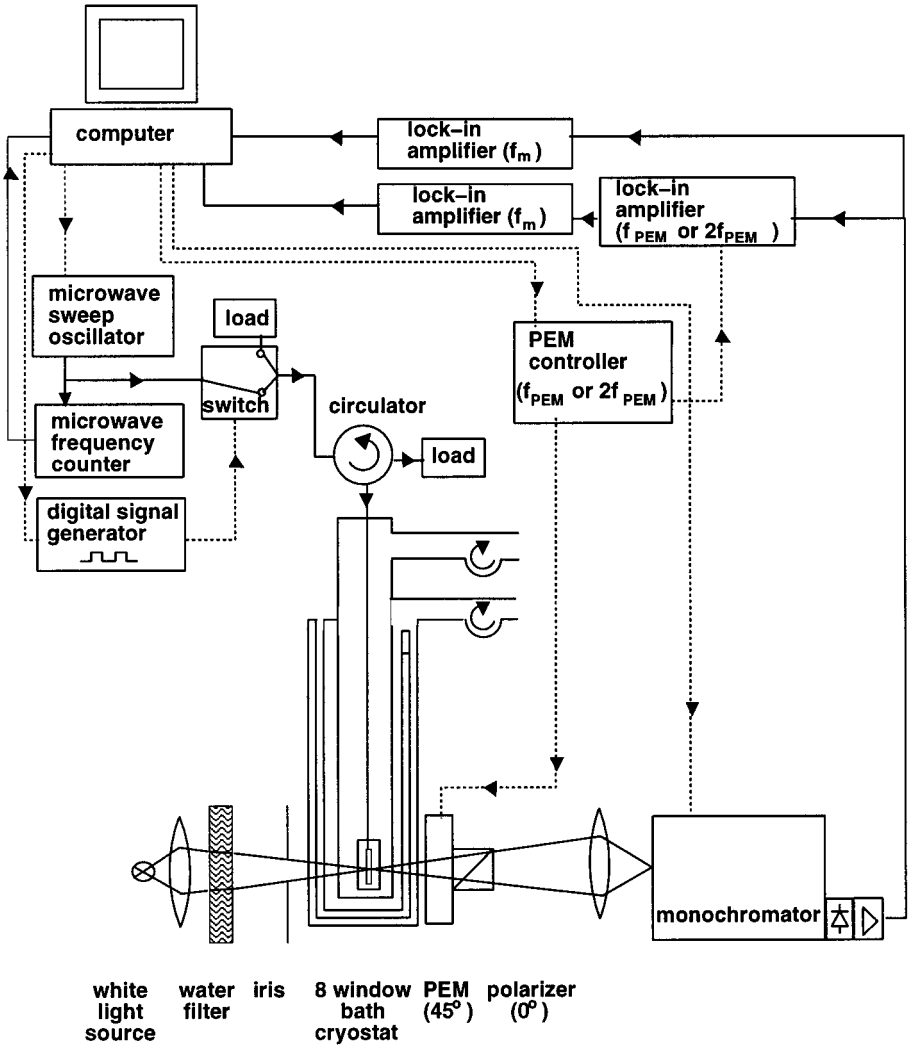

Figure 1. The LD/CD-ADMR measurement setup. The PEM controller and lock-in are set at f_{PEM} for CD-ADMR and at $2f_{PEM}$ for LD-ADMR. The signals are given with solid lines and the controls with dotted lines.

is determined by applying the appropriate operators on the incoming light vector. Mueller matrices are used rather than Jones matrices, which include the phase of the light, since our electrooptical measurement system only detects light intensities.

First, we calculate the dichroic-ADMR signal from a randomly oriented, frozen sample which, in addition to exhibiting circular dichroism and circular birefringence (CB), exhibits differences with and without the presence of a triplet state in absorbance, linear birefringence (LB), LD, CB, and CD, respectively denoted as ΔA, ΔLB, ΔLD, ΔCB, and ΔCD. Second and third, the effects of residual static birefringence in the photoelastic modulator (PEM) and a misaligned polarizer and photoelastic modulator (PEM) on the signals is calculated. Finally, the effect of strain (linear birefringence) in the windows of the sample cell and/or optical elements on the dichroic-ADMR signal is calculated. Since strain is inevitable in optics and sample cells at low temperatures, it is important to know the amount of strain tolerable in these components. All analyses include a partially polarized light source.

2.1. Experimental Setup. The LD/CD-ADMR setup is shown in Figure 1. The input beam $\bar{s}_{in}$ is produced by a tungsten−iodine lamp (250 W, 24 V), which is rotatable in the plane perpendicular to the main light propagation. The input light is focused by a lens through four quartz windows of a cryostat onto a sample in a poly(methyl methacrylate) (PMMA) cuvette. The sample is cooled to approximately 1.5 K with liquid helium to inhibit spin−lattice relaxation between spin sublevels. It is excited with a polarized magnetic field at 0°, oscillating at a microwave frequency with a square-wave modulation at frequency f_m, which is produced in a loop-gap resonator or helix connected to a HP8350A sweep oscillator with a HP8352A RF plug-in and a homebuilt digital signal generator. The light then travels through another four quartz windows of the cryostat and is focused with a lens onto a photoelastic modulator (PEM) (PEM80-FS5, HINDS International Inc., with frequency f_{PEM} = 50 kHz) at 45°, which modulates the polarization of the light at multiples of the oscillation frequency f_{PEM}. The light beam is polarized with an MGT 25 B14 Glan-Thompson prism polarizer at 0° or 90°, and the wavelength is selected with a monochromator. The optical signal is converted into an electronic one with a Peltier-cooled silicon photodiode.

The signal modulated at ($f_m + kf_{PEM}$), where k is equal to 1 for CD-ADMR and 2 for LD-ADMR, is doubly demodulated by a lock-in at kf_{PEM} followed by a lock-in at f_m (both type Stanford SR510). The signal at f_m is demodulated by one lock-in (EG&G 5209), which also is used to measure the dc signal via an A/D converter. The ΔA signal is the ratio of the signal at frequency f_m to the dc signal. The T−S spectrum is proportional to the sum of ΔA measured with the polarizer parallel to the polarization of the magnetic field and twice ΔA with the polarizer perpendicular. The LD(T−S) signal is the ratio of the signal at ($f_m + 2f_{PEM}$) to the dc signal, and the CD-

(T−S) signal is the ratio of the signal at ($f_m + f_{PEM}$) to the dc signal. The experimental setup is connected to a computer which controls the monochromator wavelength, PEM wavelength, and magnetic field frequency and records lock-in signals and experimental parameters.

In LD-ADMR the angle ϕ_i between the optical and ith microwave transition moments of the molecules in the measured sample is determined by formulas derived for photoselection:[13,14]

$$\phi_i = \arccos\left(\pm\sqrt{\frac{3R_i+1}{3-R_i}}\right) \tag{1}$$

$$R_i = \frac{\Delta LD}{\Delta A} = \frac{\Delta A_{\parallel} - \Delta A_{\perp}}{\Delta A_{\parallel} + \Delta A_{\perp}} \tag{2}$$

where $\Delta A_{\parallel}$ and $\Delta A_{\perp}$ denote the changes in absorbance parallel and perpendicular to the magnetic field. Equation 1 is valid when the power of the magnetic field is low enough such that only molecules with their magnetic transition moments parallel to the magnetic field are excited. The R-value or dichroic ratio is found from a least-squares fit to the lowest microwave power points of a plot of ΔLD versus ΔA values at a single wavelength made by measuring $\Delta A_{\parallel}$ and $\Delta A_{\perp}$ with the PEM off. Once the R-value is found at one wavelength in the spectrum, the measured spectrum with experimental gain factors can be correctly scaled to this point.

2.2. Application of Stokes−Mueller Matrix to Experimental Setup. In this section we briefly explain the Stokes−Mueller formalism, and thereafter determine a general expression for the output of the experimental setup. The Stokes vector for the ingoing lightbeam $\bar{s}_{in}$, is transformed through multiplication with a series of Mueller matrices **M**, representing the optical elements and the sample, into the Stokes vector for the output lightbeam $\bar{s}_{out}$.

$$\bar{s}_{out} = \mathbf{M}_n\mathbf{M}_{n-1}\cdots\mathbf{M}_3\mathbf{M}_2\mathbf{M}_1\bar{s}_{in} \tag{3}$$

The components of a Stokes vector are defined as follows:

$$\begin{vmatrix} s_0 \\ s_1 \\ s_2 \\ s_3 \end{vmatrix} = \begin{vmatrix} \text{the total intensity} \\ I_{45} - I_{135} \\ I_+ - I_- \\ I_0 - I_{90} \end{vmatrix} \tag{4}$$

where I_0, I_{90}, I_{45}, I_{135}, I_+, and I_- are the intensities of the light in the X, Y, 45°, 135°, right circular, and left circular directions. The magnetic field is linearly polarized in the X direction. Z is the direction of propagation of the electric field.

The Mueller matrix for a general sample can be described by **G**, which equals[15,16]

$$\mathbf{G} = e^{-\mathbf{H}} \tag{5}$$

where

$$\mathbf{H} = \begin{vmatrix} A_e & LD' & -CD & LD \\ LD' & A_e & LB & \text{CB} \\ -CD & -LB & A_e & LB' \\ LD & -CB & -LB' & A_e \end{vmatrix} \tag{6}$$

A_e, LB, LD, LB', LD', CB, and CD are defined in eq 7 in terms

$$\begin{aligned} A_e &\equiv 2.303(A_x + A_y)/2 \\ LB &\equiv (2\pi/\lambda_o)(n_x - n_y)L \\ LD &\equiv 2.303(A_x - A_y)/2 \\ LB' &\equiv (2\pi/\lambda_o)(n_{45} - n_{135})L \\ LD' &\equiv 2.303(A_{45} - A_{135})/2 \\ CB &\equiv (2\pi/\lambda_o)(n_- - n_+)L = 2\phi \\ CD &\equiv 2.303(A_- - A_+)/2 \end{aligned} \tag{7}$$

of A_x, A_y, A_{45}, A_{135}, A_+, and A_-, the absorbances in the X, Y, 45°, 135°, right and left circular polarizations, respectively; n_x, etc., are the refractive indices with the same subscript definitions; L is the path length, λ_o is the wavelength in vacuum and ϕ is the optical rotation in radians/cm.[11] In dichroic-ADMR the sample **G** is randomly oriented when the microwaves are off, thus only A_e, CD, and CB can be present with no microwaves. When the polarized microwaves are on, the signal primarily from molecules aligned with the polarized magnetic field will change because they are far more likely to get excited than molecules whose transition moment is nearly or exactly perpendicular to the magnetic field. The sample can be described using eqs 5 and 6 as

$$\mathbf{G} = e^{-(\mathbf{H}_A+\mathbf{H}_B+\mathbf{H}_C)} \tag{8}$$

where

$$\mathbf{H}_A = A_e\mathbf{I} \tag{9}$$

$$\mathbf{H}_B = \begin{vmatrix} 0 & 0 & -CD & 0 \\ 0 & 0 & 0 & CB \\ -CD & 0 & 0 & 0 \\ 0 & -CB & 0 & 0 \end{vmatrix} \tag{10}$$

$$\mathbf{H}_C = M(f_m, t) \begin{vmatrix} \Delta A & 0 & -\Delta CD & \Delta LD \\ 0 & \Delta A & \Delta LB & \Delta CB \\ -\Delta CD & -\Delta LB & \Delta A & 0 \\ \Delta LD & -\Delta CB & 0 & \Delta A \end{vmatrix} \tag{11}$$

I is the identity matrix, and $\Delta LB'$ and $\Delta LD'$ are zero due to symmetry. The term $\mathbf{H}_A$ is solely a function of the isotropic absorption A_e. The term $\mathbf{H}_B$ is only a function of the CD and CB, since the sample is assumed to be randomly oriented when no microwaves are applied. The term $\mathbf{H}_C$ is dependent on the microwave excitation, $M(f_m,t)$, which causes the changes in isotropic absorbance (ΔA), linear and circular dichroism (ΔLD, ΔCD), and linear and circular birefringence (ΔLB, ΔCB) of the sample. We assume that all matrix elements of $\mathbf{H}_B$ and $\mathbf{H}_C$ are small, and expand $e^{-(\mathbf{H}_B+\mathbf{H}_C)}$ in a Taylor's series. The sample matrix to the second order is then

$$\mathbf{G} \approx \exp(-A_e)\{\mathbf{I} - \mathbf{H}_B - \mathbf{H}_C + \mathbf{H}_B{}^2/2 + \mathbf{H}_C{}^2/(2M(f_m,t))\} \tag{12}$$

In the following discussion the approximation of **G** only to the first order is considered.

The Mueller matrix for a PEM at an angle γ, $\mathbf{B}(\gamma,\delta_o)$, is a function of the amplitude of the time-dependent retardation δ_o, and the oscillating frequency ω_{PEM} of the silica:[17]

$$\mathbf{B}(\gamma,\delta_o) = \begin{vmatrix} 1 & 0 & 0 & 0 \\ 0 & \sin^2(2\gamma) + \beta\cos^2(2\gamma) & -\mu\cos(2\gamma) & (1-\beta)\sin(4\gamma)/2 \\ 0 & \mu\cos(2\gamma) & \beta & -\mu\sin(2\gamma) \\ 0 & (1-\beta)\sin(4\gamma)/2 & \mu\sin(2\gamma) & \cos^2(2\gamma) + \beta\sin^2(2\gamma) \end{vmatrix} \quad (13)$$

The definitions and Fourier expansions of β and μ are[18]

$$\beta = \cos[\delta_o(\sin(\omega_{PEM}t)] = J_0(\delta_o) + 2\sum_{i=1}^{\infty} J_{2i}(\delta_o)\cos(2i\omega_{PEM}t) \quad (14)$$

$$\mu = \sin[\delta_o(\sin(\omega_{PEM}t)] = 2\sum_{i=1,3,5,\ldots}^{\infty} J_i(\delta_o)\cos(i\omega_{PEM}t) \quad (15)$$

where $J_i(\delta_o)$ is the Bessel function of order i, and the parameter δ_o is dependent on the power fed to the quartz piezoelectric transducer, which is mechanically coupled to the silica block. When γ is 45°, the Mueller matrix for the PEM simplifies to

$$\mathbf{B}(45°,\delta_o) = \begin{vmatrix} 1 & 0 & 0 & 0 \\ 0 & 1 & 0 & 0 \\ 0 & 0 & \beta & -\mu \\ 0 & 0 & \mu & \beta \end{vmatrix} \quad (16)$$

The Mueller matrix for a linear polarizer oriented at an angle γ under normally incident light is[11,17]

$$\mathbf{P}_\gamma = \frac{1}{2}\begin{vmatrix} 1 & \sin(2\gamma) & 0 & \cos(2\gamma) \\ \sin(2\gamma) & \sin^2(2\gamma) & 0 & \sin(4\gamma)/2 \\ 0 & 0 & 0 & 0 \\ \cos(2\gamma) & \sin(4\gamma)/2 & 0 & \cos^2(2\gamma) \end{vmatrix} \quad (17)$$

From eq 17 the Mueller matrix for a polarizer $\mathbf{P}_{0,90}$ at 0° or 90° is calculated to be (plus sign for 0°, minus sign for 90°)

$$\mathbf{P}_{0,90} = \frac{1}{2}\begin{vmatrix} 1 & 0 & 0 & \pm 1 \\ 0 & 0 & 0 & 0 \\ 0 & 0 & 0 & 0 \\ \pm 1 & 0 & 0 & 1 \end{vmatrix} \quad (18)$$

A detector acting as a partial polarizer can be described as[7,8]

$$\mathbf{D} = \begin{vmatrix} P_x^2 + P_y^2 & (P_x^2 - P_y^2)\sin(2a) & 0 & (P_x^2 - P_y^2)\cos(2a) \\ (P_x^2 - P_y^2)\sin(2a) & D_{22} & 0 & (P_x - P_y)^2\sin(4a)/2 \\ 0 & 0 & 2P_xP_y & 0 \\ (P_x^2 - P_y^2)\cos(2a) & (P_x - P_y)^2\sin(4a)/2 & 0 & D_{44} \end{vmatrix} \quad (19)$$

where

$$D_{22} = (P_x^2 + P_y^2)\sin^2(2a) + 2P_xP_y\cos^2(2a) \quad (20)$$

$$D_{44} = (P_x^2 + P_y^2)\cos^2(2a) + 2P_xP_y\sin^2(2a) \quad (21)$$

P_x^2 and P_y^2 are the principal transmittance of the detector in the X and Y directions, respectively, and a is the azimuth angle of the optical axis of the partial polarizer with respect to the X axis.

The output of the dichroic-ADMR system can be found by multiplying the matrices for the light input, sample, the PEM at 45°, the polarizer at 0° or 90°, and the partial polarizer. The Mueller matrices for the sample, PEM, polarizer, and partial polarizer were given in eqs 10−12, 16, 18, and 19.

$$\bar{S}_{out} = \frac{1}{2}\mathbf{D}\begin{vmatrix} 1 & 0 & 0 & \pm 1 \\ 0 & 0 & 0 & 0 \\ 0 & 0 & 0 & 0 \\ \pm 1 & 0 & 0 & 1 \end{vmatrix}\begin{vmatrix} 1 & 0 & 0 & 0 \\ 0 & 1 & 0 & 0 \\ 0 & 0 & \beta & -\mu \\ 0 & 0 & \mu & \beta \end{vmatrix}\cdot\mathbf{G}\cdot\begin{vmatrix} s_0 \\ s_1 \\ s_2 \\ s_3 \end{vmatrix} \quad (22)$$

Only the first element of $\bar{S}_{out}$, designated $S_{detected}$, is detected by the photodetector.

2.3. Calculation of Effects of Sample Artifacts and Partially Polarized Light Source. In this section we determine the output of the dichroic-ADMR system with a randomly oriented sample with CD, CB, and all of the magnetic field dependent optical properties, ΔA, ΔLB, ΔLD, ΔCB, and ΔCD. We define the constant $F \equiv \exp(-A_{iso})[(P_x^2 + P_y^2) \pm (P_x^2 - P_y^2)\cos(2a)]$, where A_{iso} is the total isotropic absorbance of the system. Throughout this section the top and bottom of the plus or minus sign will refer to the polarizer at 0° and 90°, respectively. Using eqs 10−12, 16, 19, and 22 the signals at each frequency can be derived:

$$\text{dc signal} = \frac{F}{2}[s_0 + s_2CD \pm (s_1CB + s_3)J_0(\delta_o)]$$

$$\text{ac signal}(f_m) = -0.5F[s_0\Delta A - s_2\Delta CD + s_3\Delta LD \pm J_0(\delta_o)(s_0\Delta LD - s_1\Delta CB + s_3\Delta A)]$$

$$\text{ac signal}(kf_{PEM}) = \pm FJ_k(\delta_o)s_{eo}$$

$$\text{ac signal}(f_m,f_{PEM}) = \pm FJ_1(\delta_o)(s_0\Delta CD + s_1\Delta LB - s_2\Delta A)$$

$$\text{ac signal}(f_m,2f_{PEM}) = \pm FJ_2(\delta_o)(-s_0\Delta LD + s_1\Delta CB - s_3\Delta A) \quad (23)$$

where k is an integer and s_{eo} is equal to $(s_0CD + s_2)$ when k is odd and $(s_1CB + s_3)$ when k is even.

From eq 23 we derive the measured R-value, and the ΔA, ΔLD, and ΔCD spectra. We define $K \equiv s_0\Delta LD - s_1\Delta CB + s_3\Delta A$.

$$\Delta A|_{meas} = \frac{AC(f_m)}{DC} = \frac{-[s_0\Delta A - s_2\Delta CD + s_3\Delta LD \pm J_0(\delta_o)K]}{[s_0 + s_2CD \pm (s_1CB + s_3)J_0(\delta_o)]} \quad (24)$$

$$\Delta LD|_{meas} = \frac{AC(f_m,2f_{PEM})}{DC} = \pm 2J_2(\delta_o)\frac{-s_0\Delta LD + s_1\Delta CB - s_3\Delta A}{[s_0 + s_2CD \pm (s_1CB + s_3)J_0(\delta_o)]} \quad (25)$$

$$\Delta CD|_{meas} = \frac{AC(f_m,f_{PEM})}{DC} = \pm 2J_1(\delta_o)\frac{(s_0\Delta CD + s_1\Delta LB - s_2\Delta A)}{[s_0 + s_2CD \pm (s_1CB + s_3)J_0(\delta_o)]} \quad (26)$$

$$R_{meas} = \left.\frac{\Delta LD}{\Delta A}\right|_{meas} = \pm 2J_2(\delta_o)\frac{(s_0\Delta LD - s_1\Delta CB + s_3\Delta A)}{[s_0\Delta A - s_2\Delta CD + s_3\Delta LD \pm J_0(\delta_o)K]} \quad (27)$$

In eqs 24−27 the signals are the sum of more than one absorbance variable (ΔA, ΔCD, ΔLD, etc.). They can be

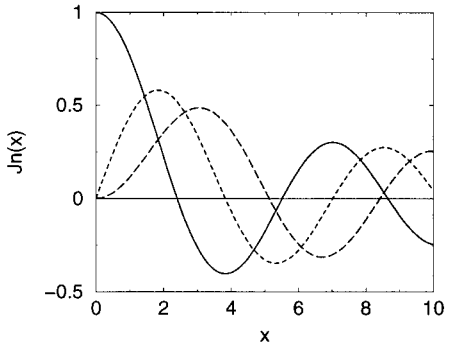

Figure 2. The zero, first, and second order Bessel functions $J_n(x)$ as a function of the argument x, in solid, dashed, and long-dashed lines, respectively.

simplified by (1) reduction of the PEM modulation amplitude to $\delta_o = 0.76\pi$ and (2) minimization of the proportion of LD in the source light ($|s_3|/s_0$) through lamp rotation.

First, by reducing the voltage sent to the PEM to 76% of its usual setting, the argument of the Bessel function of zero order, $J_0(\delta_o)$, is set to 0.76π making $J_0(\delta_o) \approx 0$, as shown in the plot of the zero-order Bessel function in Figure 2. This procedure is well-known to researchers determining Mueller matrix elements.[7,8,9,12,19] This sets $J_0(\delta_o)$ to zero in eq 23 in the dc signal and ac signal(f_m) and in eqs 24−27. Additionally the CD(T−S) signal increases by 82% and the LD(T−S) signal decreases 11%, due to the changes in the magnitudes of the first- and second-order Bessel functions, as shown in Figure 2 and in eqs 25 and 26. Alternatively, $J_0(\delta_o)$ can be kept nonzero, and the ΔA component of the dichroic ratio R can be corrected afterward for the extra $J_0(\delta_o)\Delta LD$ term in the denominator of eq 27 as in ref 20. With a nonzero $J_0(\delta_o)$ the ΔA spectrum recorded simultaneously with the LD(T−S) spectrum then also needs correction for the extra $J_0(\delta_o)\Delta LD$ wavelength-dependent term.

In Figure 3A−C the ΔA spectra and in Figures 3D−F the LD(T−S) spectra of the reaction centers (RCs) of the purple photosynthetic bacterium *Rb. sphaeroides* R26 recorded with the polarizer perpendicular (dashed line) and parallel (solid line) to the magnetic field are presented for three different settings of the PEM retardation δ_o. In Figure 3A,D, $\delta_o = 0.76\pi$; in Figure 3B,E, $\delta_o = \pi$; in Figure 3C,F, $\delta_o = 1$. The difference between the orthogonally recorded ΔA spectra (dotted line) is greatest for $\delta_o = 1$ and is least for $\delta_o = 0.76\pi$, in agreement with eq 24, which states that the difference of the two signals should be proportional to $J_0(\delta_o)$ (assuming $s_3 J_0(\delta_o)/s_0 \ll 1$). Additionally, the experimental ratio of the measured difference between the orthogonally recorded ΔA spectra for $\delta_o = 1$ and $\delta_o = \pi$ agrees with the theoretically determined ratio $J_0(1)/J_0(\pi)$. The sum of the LD(T−S) spectra in Figure 3D−F is approximately 0 for all δ_o settings, as expected from eq 25 since the signals in the two polarizer positions only differ by a factor −1.

In Figure 4 the difference of the orthogonally recorded ΔA spectra for $\delta_o = 1$ is compared to the LD(T−S) signal. The $J_0(1)$ spectrum is chosen since $|J_0(1)| > |J_0(\pi)| > |J_0(0.76\pi)|$. The ΔA spectra difference is indeed very close to the LD(T−S) signal, indicating that $\Delta LD \gg (-s_1 \Delta CB/s_0 + s_3 \Delta A/s_0)$ in the expected difference. The predominance of ΔLD in the ΔA spectra difference rests upon the assumption that the LD(T−S) signal is pure, which is highly likely since it is reproducible on trials with different amounts of s_1 and s_3.

The second method to purify the signals in eqs 24−27 is to minimize the relative amount of LD in the light source $|s_3|/s_0$ using the ratio of the ac signal($2f_{PEM}$) to the dc signal, which

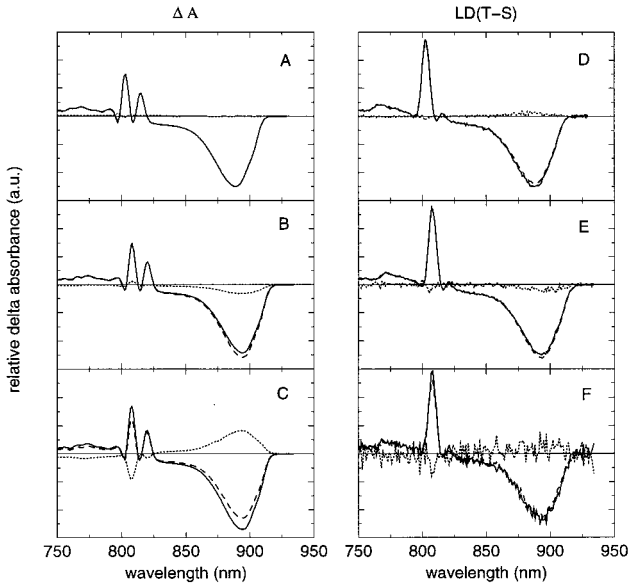

Figure 3. (A−C) ΔA spectra and (D−F) LD(T−S) spectra of RCs of the purple photosynthetic bacterium *Rb. sphaeroides* R26 with the polarizer oriented parallel (solid line) and perpendicular (dashed line) to the magnetic field. Three different settings of the PEM retardation δ_o are shown. In (A) and (D), $\delta_o = 0.76\pi$; in (B) and (E), $\delta_o = \pi$; in (C) and (F), $\delta_o = 1$. The microwave frequency lies in the $|D|-|E|$ transition (467 MHz) of the triplet. The LD(T−S) signal for the parallel polarizer orientation is multiplied by −1, for easier comparison with the perpendicular polarizer orientation signal. The difference (sum) between the orthogonally recorded ΔA (LD(T−S)) spectra is shown with the dotted line, enlarged by a factor of 2.

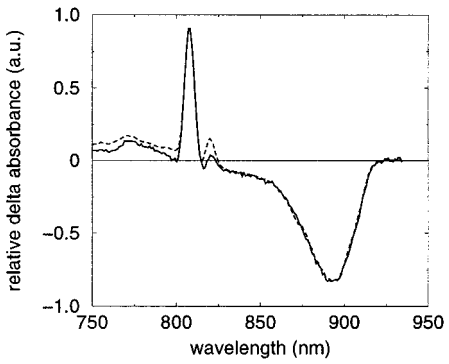

Figure 4. Sum of the ΔA spectra of RCs of the purple photosynthetic bacterium *Rb. sphaeroides* R26 with the polarizer oriented parallel and perpendicular to the magnetic field (dotted line) compared with the LD(T−S) spectrum (solid line). The PEM retardance δ_o is set to 1 in the ΔA spectra and to 0.76π in the reference LD(T−S) spectra (for high purity).

according to eq 23 is

$$\frac{\text{ac signal}(2f_{PEM})}{\text{dc signal}} = \pm \frac{2(s_1 CB + s_3) J_2(\delta_o)}{s_0 + s_2 CD \pm (s_1 CB + s_3) J_0(\delta_o)} \qquad (28)$$

It is best to set the light with no sample present so that CB and CD are zero. Alternatively one could use a wavelength with no CB. The ratio $|s_3|/s_0$ is minimized by first setting the PEM so that $J_0(\delta_o)$ is zero and then rotating the light source until the value of the ratio is minimized.

In Figure 5A the ΔA spectra and in Figure 5B LD(T−S) spectra are shown for one lamp position in which the ratio $|s_3|/s_0$ is minimized (dot−dashed line) and one in which it is not minimized (solid line). The ratio of the ac signal($2f_{PEM}$) to the dc signal was minimized with the sample present. The ΔA

spectra in Figure 5A for the two lamp positions are identical. Since the signal for ΔA spectra with $J_0(\delta_o) \approx 0$ is $(\Delta A - s_2\Delta CD/s_0 + s_3\Delta CD/s_0 + s_3\Delta LD/s_0)$, we can conclude that the ΔA term dominates. The LD(T−S) spectra in Figure 5B are very different from each other. According to eq 25 the measured LD(T−S) signal is equal to $(\Delta LD - s_1\Delta CB/s_0 + s_3\Delta A/s_0)$. Experimentally we see, in Figure 5B, that the sum of the true LD(T−S) and (ΔA) spectra (dot−dashed and dashed lines, respectively) does give an excellent fit (dotted line) of the measured LD(T−S) spectrum with the lamp in an unsuitable position. We thus conclude that the $s_1\Delta CB/s_0$ term is unimportant at these wavelengths.

Note that the light intensity factor s_1 is maximized when $|s_3|$ is minimized (eq 4) but the tradeoff is worthwhile in light of eq 25 since $\Delta CB < \Delta A$. It is only disadvantageous in eq 26 in the $\Delta CD|_{meas}$ term since $s_1\Delta LB$ is increased. Minimization, however, of s_3 is actually not necessary in ΔCD measurements because in eq 26 only $s_3J_0(\delta_o)$ appears, which can be set to zero. Alternatively, s_1 can be minimized for CD(T−S) measurements by maximizing s_3.

After minimizing $|s_3|/s_0$ and setting $J_0(\delta_o)$ to zero, eqs 24−27 reduce to

$$\Delta A|_{meas} \approx -\Delta A \quad \text{when} \left|\frac{-s_2\Delta CD + s_3\Delta LD}{s_0\Delta A}\right| \ll 1 \text{ and } \left|\frac{s_2CD}{s_0}\right| \ll 1$$

$$\Delta LD|_{meas} \approx \mp 2J_2(\delta_o)\Delta LD \quad \text{when} \left|\frac{-s_1\Delta CB + s_3\Delta A}{s_0\Delta LD}\right| \ll 1 \text{ and } \left|\frac{s_2CD}{s_0}\right| \ll 1$$

$$\Delta CD|_{meas} \approx \pm 2J_1(\delta_o)\Delta CD \quad \text{when} \left|\frac{-s_1\Delta LB + s_2\Delta A}{s_0\Delta CD}\right| \ll 1 \text{ and } \left|\frac{s_2CD}{s_0}\right| \ll 1 \quad (29)$$

$$R|_{meas} \propto \Delta LD/\Delta A \quad \text{when} \left|\frac{-s_1\Delta CB + s_3\Delta A}{s_0\Delta LD}\right| \ll 1 \text{ and } \left|\frac{-s_2\Delta CD + s_3\Delta LD}{s_0\Delta A}\right| \ll 1 \quad (30)$$

The exact *R*-ratio can be measured by calibrating the instrument to account for the gain constants; otherwise the *R*-ratio without the gain factor can be measured with one lock-in amplifier with the PEM off at a given microwave power using

$$R_{meas} = \left.\frac{\Delta LD}{\Delta A}\right|_{meas} = \frac{\left.\frac{AC(f_m,PEM_{off})}{DC(PEM_{off})}\right|_{||} - \left.\frac{AC(f_m,PEM_{off})}{DC(PEM_{off})}\right|_{\perp}}{\left.\frac{AC(f_m,PEM_{off})}{DC(PEM_{off})}\right|_{||} + \left.\frac{AC(f_m,PEM_{off})}{DC(PEM_{off})}\right|_{\perp}} \quad (31)$$

where

$$\frac{AC(f_m,PEM_{off})}{DC(PEM_{off})} \approx -(\Delta A \pm \Delta LD) \quad (32)$$

with the plus sign for the parallel polarizer position and the minus sign for the perpendicular polarizer position. Equation 31 will reduce to eq 30 assuming that $s_2CD \pm (s_1CB + s_3) \ll s_0$ in addition to the same conditions as in the other method of measuring *R* (eq 30).

In Figures 4 and 5 we have shown the validity of the approximations in eqs 29 and 30 for $\Delta A|_{meas}$, $\Delta LD|_{meas}$, and $R|_{meas}$ in the case of RCs of the photosynthetic bacterium *Rb. sphaeroides* R26. In order to check if the conditions are satisfied more generally, we need to estimate the relative magnitude of the measured values of optical anisotropies. For partially oriented systems $A_e > 10LD$ and $A_e > (10^3-10^5)CD$.[11,21] In the region of an absorption band CB is usually of the same order of magnitude as CD,[11] but LB can be 10 times more than LD[22] particularly for oriented polymer systems where form birefringence, solvent ordering, and other effects contribute, which have nothing to do with the chromophore under investigation.[11] Thus, for systems where the background effects are minor, reasonable estimates of the microwave-independent optical parameters are $A_e = 2-4$, $LD \cong LB = 0.2$, and $CD = CB = 10^{-3}-10^{-5}$.[11] We assume that the differences in these anisotropies between the triplet and singlet states (ΔA, ΔLB, ΔLB, ΔCD, ΔCB) have the same relative order of magnitudes. Furthermore, we know that $s_0^2 \geq (s_1^2 + s_2^2 + s_3^2)$ and assume that the light source is primarily unpolarized light. Using these limitations we conclude that our approximations of $\Delta A|_{meas}$, $\Delta LD|_{meas}$, $\Delta CD|_{meas}$, and $R|_{meas}$ in eqs 29 and 30 are widely valid.

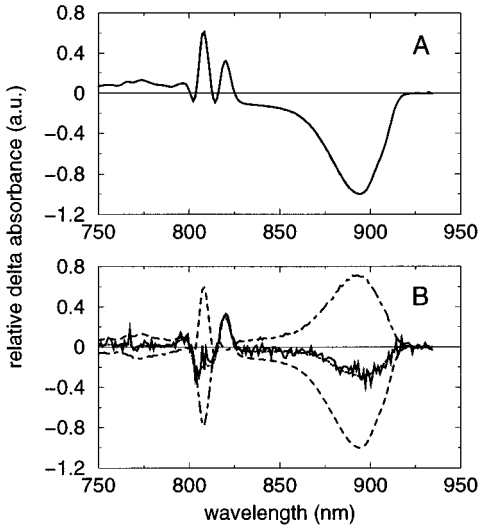

Figure 5. Comparison of the ΔA (A) and LD(T−S) spectra (B) with light in optimized (dot−dashed line) and unoptimized (solid line) positions. Additionally in (B), the dashed line is ΔA with light in optimized position; dotted line is fit of LD(T−S) spectrum in unoptimized position with a sum of the optimized LD(T−S) and ΔA spectra presented in (B).

2.4. Residual Static Birefringence of PEM. The PEM can have a small, time-independent, residual static birefringence $\alpha(\lambda)$, which will change its retardation from δ_o to $(\delta_o + \alpha(\lambda))$.[23] This will cause mixing of the signals because the cosine (sine) of the retardance will additionally include odd (even) frequency components. Using eqs 10−12, 16, 19, and 22, the measured ΔA, ΔLD, and ΔCD can be derived (with $J_0(\delta_o) \approx 0$, $\cos(\alpha(\lambda)) \approx 1$):

$$\Delta A|_{meas} \approx -\Delta A$$

$$\Delta LD|_{meas} \approx \mp 2J_2(\delta_o)\Delta LD$$

$$\Delta CD|_{meas} \approx \pm 2J_1(\delta_o)\{\Delta CD - \Delta LD \sin(\alpha(\lambda))\} \quad (33)$$

The $\Delta A|_{meas}$ in eq 33 is valid under the same conditions as for $\Delta A|_{meas}$ in eq 29. For the ΔLD_{meas} and $\Delta CD|_{meas}$ approximations in eq 33 to be valid, they must satisfy both the $\Delta LD|_{meas}$ and $\Delta CD|_{meas}$ requirements in eq 29 and additionally $|\Delta CD/\Delta LD|$

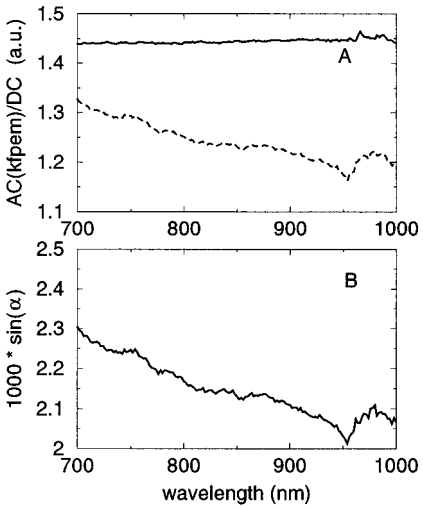

Figure 6. (A) $AC(f_{PEM})/DC$ signal (dashed) magnified by a factor of 400, $AC(2f_{PEM})/DC$ signal (solid) versus wavelength, both divided by their corresponding Bessel functions. (B) Function $\sin(\alpha(\lambda))$, a.u.

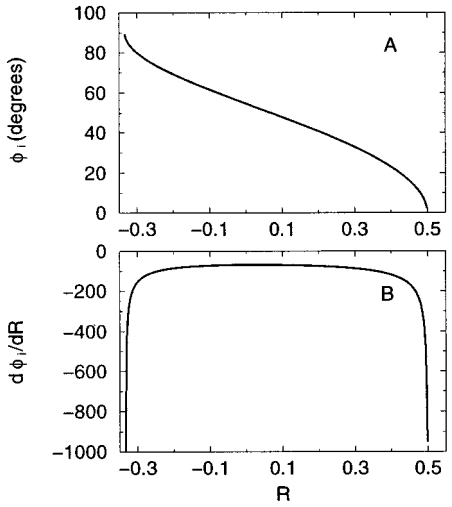

Figure 7. Angle ϕ_i between the optical and ith microwave transition moments versus R (A), and the derivative of ϕ_i versus R (B).

$\ll 1$. From this analysis we conclude that the residual static birefringence of the PEM can cause ΔLD to enter into the ΔCD measurements.

By placing the PEM at 45° between two crossed polarizers at 90° and 0°, we can measure the residual static birefringence $\alpha(\lambda)$. Assuming $CB = CD = 0$ and $s_2 \ll s_3 \sin(\alpha(\lambda))$

$$\frac{AC(f_{PEM})}{DC} = \mp 2J_1(\delta_o)\sin(\alpha(\lambda))$$

$$\frac{AC(2f_{PEM})}{DC} = \mp 2J_2(\delta_o) \qquad (34)$$

In Figure 6 the experimental $AC(f_{PEM})/DC$ and $AC(2f_{PEM})/DC$ signals and the derived function $\sin(\alpha(\lambda))$ are shown. The $AC(2f_{PEM})/DC$ signal is larger than the $AC(f_{PEM})/DC$ signal because it is not multiplied by $\sin(\alpha(\lambda))$, which is very small and decreases at longer wavelengths. We estimate the value of $\sin(\alpha(\lambda))$ to be less than or equal to 3×10^{-3} in the 700−1000 nm range. The qualitative and quantitative character of $\alpha(\lambda)$ agrees with that of ref 7. Using our estimates for ΔLD and ΔCD from section 2.3, we estimate $(\Delta LD/\Delta CD)\sin(\alpha(\lambda)) \approx (10^2-10^4)(3 \times 10^{-3}) = 0.3-3$. Thus even with an excellent PEM with a residual static birefringence much smaller than 1°, there may be a significant contribution of ΔLD in the ΔCD signal.

The measured CD(T−S) spectra can be corrected for the LD-(T−S) contribution by using the measured CD(T−S) spectra of the same selected subset of molecules in two different microwave transitions of the triplet. The CD(T−S) spectra of the two microwave transitions should have approximately the same shape. The spectra measured in the two transitions can be normalized at points where the LD(T−S) spectra are approximately zero, to set the CD(T−S) contribution the same. The LD(T−S) spectra for the respective transitions can then be subtracted from the measured CD(T−S) spectra until the CD-(T−S) spectra from the two transitions are the same.

2.5. Misplacement of Polarizer and PEM by an Angle dθ. Another source of error in the LD-ADMR measurements may be misplacement of the PEM and polarizer by an angle dθ. The output of the system before the photodetector is calculated to be

$$\bar{S}_{out}(d\theta) = \mathbf{D}\cdot\mathbf{P}_{0,90+d\theta}\cdot\mathbf{B}(45+d\theta,\delta_o)\cdot\mathbf{G}\cdot\begin{vmatrix} s_0 \\ s_1 \\ s_2 \\ s_3 \end{vmatrix} \qquad (35)$$

From eqs 10−12, 16, 19, and 35 we can derive the signals at each frequency, with $J_0(\delta_o)$ set to zero:

$$\Delta A|_{meas} \approx -\Delta A \qquad (36)$$

$$\Delta LD|_{meas} \approx \mp 2J_2(\delta_o)\{\cos(2\,d\theta)\Delta LD + \sin(2\,d\theta)s_1\Delta A/s_0\} \qquad (37)$$

$$\Delta CD|_{meas} \approx \pm 2J_1(\delta_o)\Delta CD \qquad (38)$$

We assume all conditions in eq 29 are valid and additionally for $\Delta LD|_{meas}$ that $(s_2\Delta LB + s_3\Delta CB)/(s_1\Delta A) \ll 1$. The only term in the above equations which is different from eq 29 is the one for $\Delta LD|_{meas}$. The amount of ΔA in the measured ΔLD signal is minor because ΔLD is about 1 order of magnitude smaller than ΔA whereas $s_1 \sin(2\,d\theta) \approx 10^{-3}$. The relative change $\Delta LD|_{meas}$ for small dθ is equal to the change in the dichroic ratio δR:

$$\frac{\delta R}{R} \approx \sin(2\,d\theta)\frac{s_1}{s_0 R} \qquad (39)$$

The severity of the corruption to the ΔLD and dichroic ratio signals is directly proportional to the angle of misplacement, the relative amount of 45° polarization of the light source, and the inverse of the dichroic ratio. We estimate the error in the angle to be at most 3°, for which $\sin(2\,d\theta) = 0.1$. An upper limit of the relative amount of 45° polarization of the light source is estimated at 10%. Thus, although the relative change in R will be greatest around $R = 0$, the change in the angle ϕ will be largest when R enters the extremities of the ϕ-curve, namely, when $R \approx -0.3$ or when $R \approx 0.5$, as shown in Figure 7. Nevertheless, the error in ϕ_i is probably less than 5°. At the extremities of the ϕ-curve, ϕ should already be determined with another method, regardless of a misplacement of the PEM and polarizer.

2.6. Calculation of Effects of Strain in Cryostat Windows/Cell. Strain is always present in optical elements and is even

more noticeable at low temperatures. In this section we will consider the effect on the output signal of low levels of LB and LD in the optical components neighboring the sample. Circular anisotropies in optical components are neglected since they are usually too small to contribute to significant errors.[12] With the use of eqs 5, 6, and 12 the small-signal matrix for a nonideal optical component is found to be (ignoring the attenuation factor)

$$\mathbf{OP}_i = \begin{vmatrix} 1 & -a_i' & 0 & -a_i \\ -a_i' & 1 & -b_i & 0 \\ 0 & b_i & 1 & -b_i' \\ -a_i & 0 & -b_i' & 1 \end{vmatrix} \tag{40}$$

where a_i, a_i', b_i, and b_i' represent the amounts of *LD*, *LD*′, *LB*, and *LB*′, respectively. When nonideal optical element with Mueller matrices $\mathbf{OP}_i$ are present before and after the sample, the system output will be

$$\bar{S}_{\text{out}} = \frac{1}{2}\mathbf{D}\begin{vmatrix} 1 & 0 & 0 & \pm 1 \\ 0 & 0 & 0 & 0 \\ 0 & 0 & 0 & 0 \\ \pm 1 & 0 & 0 & 1 \end{vmatrix}\begin{vmatrix} 1 & 0 & 0 & 0 \\ 0 & 1 & 0 & 0 \\ 0 & 0 & \beta & -\mu \\ 0 & 0 & \mu & \beta \end{vmatrix}\cdot\mathbf{OP}_2\cdot\mathbf{G}\cdot\mathbf{OP}_1\cdot\begin{vmatrix} s_0 \\ s_1 \\ s_2 \\ s_3 \end{vmatrix} \tag{41}$$

Using eqs 10−12, 16, 18, 19, 40, and 41, under assumption that s_1, s_2, s_3, a_i, a_i', b_i, b_i', *LB*, and *CB* are second-order terms, and keeping only first- and second-order terms for each expression, with $J_0(\delta_o) \approx 0$, we derive the measured ΔA, ΔLD, and ΔCD signals:

$$\Delta A|_{\text{meas}} \approx -{s_0}^{-1}\{s_0\Delta A - s_2\Delta CD + \Delta LD[-s_0(a_1 + a_2) + s_3]\} \tag{42}$$

$$\Delta LD|_{\text{meas}} \approx \mp 2J_2(\delta_o)\{\Delta A[-(a_1 + a_2) + s_3/s_0] + \Delta LD - b_2'\Delta CD\} \tag{43}$$

$$\Delta CD|_{\text{meas}} = \mp 2J_1(\delta_o)\{s_2\Delta A/s_0 - \Delta CD + \Delta LB(a_1' - s_1/s_0) - \Delta LD b_2'\} \tag{44}$$

The ac signal at the multiples of the fundamental PEM frequency is

$$AC(kf_{\text{PEM}})/DC = \pm FJ_k(\delta_o)s_{eo} \tag{45}$$

where k is an integer, and

$$s_{eo} = \begin{cases} s_0CD + s_1[b_1 + b_2] + s_2 - s_3[b_1' + b_2'] & k \text{ odd} \\ -s_0[a_1 + a_2] + s_1CB + s_2[b_1' + b_2'] + s_3 & k \text{ even} \end{cases}$$

The mechanically induced strain of the cryostat windows, which causes an extra linear dichroism component at 0, $2f_{\text{PEM}}$, $4f_{\text{PEM}}$, etc., as seen in eq 45, was also found in ref 20. However, these authors did not address the possibility of these linear dichroic components being present in the measured ΔLD signal (eq 43). The primary interfering terms in the measured ΔLD spectra will be the total residual linear dichroism times the ΔA signal. However, the residual linear dichroism would need to be unreasonably large (on the order of 0.01) to cause interference. There will be no difficulties in measuring the ΔA spectra in the presence of strain in the cell windows. For the ΔCD spectra mainly $b_2'\Delta LD$ or $a_1'\Delta LB$ signals could cause contamination. The conditions under which the measured signals reduce to eq 29 are

$$\Delta A|_{\text{meas}} \approx -\Delta A \quad \text{when} \left|\frac{-s_2\Delta CD + \Delta LD[-s_0(a_1 + a_2) + s_3]}{s_0\Delta A}\right| \ll 1$$

$$\Delta LD|_{\text{meas}} \approx \mp 2J_2(\delta_o)\Delta LD \quad \text{when} \left|\frac{\Delta A[-s_0(a_1 + a_2) + s_3] - \Delta CD s_0 b_2'}{\Delta LD s_0}\right| \ll 1$$

$$\Delta CD|_{\text{meas}} \approx \pm 2J_1(\delta_o)\Delta CD \quad \text{when} \left|\frac{\Delta A s_2 + \Delta LB(s_0 a_1' - s_1) - \Delta LD s_0 b_2'}{-\Delta CD s_0}\right| \ll 1 \tag{46}$$

2.7. Reducing Birefringence in Cryostat Windows/Sample Cell. From eqs 43 and 44 we can draw two major conclusions:

1. ΔA could be in the $\Delta LD|_{\text{meas}}$ signal if the sum of the linear dichroism in all the optical elements (besides the sample) before the polarizer is large enough.

2. ΔLD could be in the $\Delta CD|_{\text{meas}}$ signal if the linear birefringence of the optical elements between the sample and the polarizer is large enough.

To ensure that the level of linear dichroism and linear birefringence in the optical elements is as low as possible, we have developed two techniques to measure these quantities. In the first technique we measure the amount of this background linear dichroism by adding a polarizer at 45° after the light source, to convert incoming light to the Stokes vector $0.5(s_0 + s_1)[1, 1, 0, 0]$. We then substitute $0.5(s_0 + s_1)$ for s_0 and s_1 and 0 for s_2 and s_3 in eq 45, and remove the sample from the sample cell, to obtain

$$AC(2f_{\text{PEM}})/DC \approx \mp 4J_2(\delta_o)(a_1 + a_2) \tag{47}$$

With this method we can try various optical components and choose the ones with the smallest amount of linear dichroism. Alternatively, we can omit the extra polarizer at 45° and minimize the effect of the linear dichroism present in the optical elements by rotating the lamp and minimizing the signal $AC(2f_{\text{PEM}})/DC$ with the sample present.

$$AC(2f_{\text{PEM}})/DC \approx \pm 4{s_0}^{-1}J_2(\delta_o)\{-s_0[a_1 + a_2] + s_1CB - s_2[b_1' + b_2'] + s_3\} \tag{48}$$

Then when $AC(2f_{\text{PEM}})/DC$ is minimized, ${s_0}^{-1}(-s_0(a_1 + a_2) + s_3)$ will be minimized.

In the second technique the linear birefringence in the optical elements between the sample and polarizer is minimized. A polarizer at 0° is used after the light source to convert the input light vector to $0.5(s_0 \pm s_3)[1, 0, 0, \pm 1]$. Then from eq 45

$$\frac{AC(f_{\text{PEM}})}{DC} \approx \pm 4J_1(\delta_o)[CD - (b_1' + b_2')] \tag{49}$$

We assume that the CD of the cuvette ≈ 0, and test one side of the sample cell at a time (so $b_1' \approx 0$) by rotating it until b_2' is a minimum. A disadvantage to this procedure is that it works well for testing cuvettes but is not practical for testing half the windows in the cryostat. Since we do not want to test the sum of the linear birefringences of the cryostat, it is not currently

experimentally possible to test only the linear birefringence between the sample and the polarizer at low temperatures.

3. Conclusions

In order to improve the sensitivity and reliability of our dichroic-ADMR measurements, we have developed a list of procedures to ensure signal purity and high signal to noise ratio:

1. reduction of the modulation amplitude of the PEM to $\delta_o = 0.76\pi$

2. minimization of the relative LD in the light source, $|s_3|/s_0$, through lamp rotation

3. minimization of the sum of the linear dichroism of the optical elements before the polarizer ($a_1 + a_2$) through minimization of the ratio $AC(2f_{PEM})/DC$ between polarizers with relative angle 45°

4. minimization of the linear birefringence b_2' in the optical elements between the sample and the polarizer

5. use of PEM with the lowest residual static birefringence possible

The only drawback with the measurement of the linear birefringence b_2' is that it cannot be accurately measured at low temperatures and can only be measured at room temperatures for the cuvette.

Even with the use of our procedures, there are a number of caveats in measuring the various types of T−S signals. Through use of the Stokes−Mueller formalism, we have shown that the ΔA signal can be accurately measured regardless of a PEM with a residual static birefringence, a misplaced polarizer and PEM by a small angle, or anisotropies in the optical elements. The introduction of ΔA in the $\Delta LD|_{meas}$ signal due to the sum of the linear dichroism in all the optical elements (besides the sample) before the polarizer is unlikely. The misplaced polarizer and PEM will change the measured angle between the optical and microwave transition moments by at most 5°, and will add a negligible amount of ΔA in the ΔLD signal. A contribution from ΔLD could be in the $\Delta CD|_{meas}$ signal if the linear birefringence of the optical elements between the sample and the polarizer times the ΔLD signal is on the order of the ΔCD signal. The contamination of the measured ΔCD signal by the ΔLD signal due to the residual static birefringence of the PEM is nonnegligible even for excellent quality PEMs. It can be corrected for by recording the ΔCD signal at two different transitions, for example, the $|D| \pm |E|$ ODMR transitions.

Acknowledgment. This work was supported by the Chemical Science Section of the Netherlands' Organization for Scientific Research (NWO). We are grateful to S. Jansen for preparation of isolated R26 RCs.

References and Notes

(1) Maki, A. H. In *Biological Magnetic Resonance*; Berliner, L. J., Reuben, J., Eds.; Plenum Press: New York, 1984; Vol. 6, p 187.

(2) Hoff, A. J. In *Advanced EPR: Applications in Biology and Biochemistry*; Hoff, A. J., Ed.; Elsevier: Amsterdam, 1989; p 633.

(3) Lous, E. J.; Hoff, A. J. *Proc. Natl. Acad. Sci. U.S.A.* **1987**, *84*, 6147.

(4) Van der Vos, R.; Hoff, A. J. *Appl. Magn. Reson.* **1991**, *2*, 179.

(5) Vrieze, J.; Hoff, A. J. *Biochim. Biophys. Acta* **1996**, *1276*, 210.

(6) Louwe, R. J. W.; Vrieze, J.; Aartsma, T. J.; Hoff, A. J. *J. Phys. Chem. B* **1997**, *101*, 11273.

(7) Shindo, Y.; Nakagawa, M. *Rev. Sci. Instrum.* **1985**, *56*, 32.

(8) Shindo, Y.; Ohmi, Y. *J. Am. Chem. Soc.* **1985**, *107*, 91.

(9) Shindo, Y.; Nishio, M.; Maeda, S. *Biopolymers* **1990**, *30*, 405.

(10) Björling, S. C.; Goldbeck, R. A.; Milder, S. J.; Randall, C. E.; Lewis, J. W.; Kliger, D. *S. J. Phys. Chem.* **1991**, *95*, 4685.

(11) Schellman, J.; Jensen, H. P. *Chem. Rev.* **1987**, *87*, 1359.

(12) Schellman, J. A. In *Polarized Spectroscopy of Ordered Systems;* Samori, B., Thulstrup, E. W., Eds.; Kluwer Academic Publishers: Dordrecht, 1988; p 231.

(13) Verméglio, A.; Breton, J.; Paillotin, G.; Cogdell, R. *Biochim. Biophys. Acta* **1978**, *501*, 514.

(14) Meiburg, R. F. Ph.D. Thesis, Leiden University, The Netherlands, 1985.

(15) Gō, N. *J. Phys. Soc. Jpn.* **1967**, *23*, 88.

(16) Jensen, H. P.; Schellman, J. A.; Troxell, T. *Appl. Spectrosc.* **1978**, *32*, 192.

(17) Davidsson, A.; Nordén, B. *Spectrochim. Acta* **1976**, *32A*, 717.

(18) Abramowitz, M., Stegun, I. A., Eds.; *Handbook of Mathematical Functions with Formulas, Graphs, and Mathematical Tables*; Dover Publications, Inc.: New York, 1970.

(19) Dunlap, D.; Samori, B.; Bustamante, C. In *Polarized Spectroscopy of Ordered Systems*; Samori, B., Thulstrup, E. W., Eds.; Kluwer Academic Publishers: Dordrecht, 1988; p 275.

(20) Louwe, R. J. W.; Vrieze, J.; Aartsma, T. J.; Hoff, A. J. *J. Phys. Chem. B* **1997**, *101*, 11280.

(21) Lewis, J. W.; Tilton, R. F.; Einterz, C. M.; Milder, S. J.; Kuntz, I. D.; Kliger, D. S. *J. Phys. Chem.* **1985**, *89*, 289.

(22) Shindo, Y.; Nishio, M. *Biopolymers* **1990**, *30*, 25.

(23) Shindo, Y.; Mizuno, K.; Sudani, M.; Hayakawa, H.; Ohmi, Y.; Sakayanagi, N.; Takeuchi, N. *Rev. Sci. Instrum.* **1989**, *60*, 3633.

(24) Abbreviations: LB, linear birefringence; LD, linear dichroism; CB, circular birefringence; CD, circular dichroism; T−S triplet-minus-singlet; ODMR, optically detected magnetic resonance; ADMR, absorbance-detected magnetic resonance; PDMR, phosphorescence-detected magnetic resonance; FDMR, fluorescence-detected magnetic resonance; RC, reaction center; PEM, photoelastic modulator; PMMA, poly(methyl methacrylate).